Title

Time reversal symmetry breaking and odd viscosity in active fluids: Green–Kubo and NEMD results

Journal

The Journal of Chemical Physics, 152(20)

ISSN

0021-9606

Authors

Hargus, Cory
Klymko, Katherine
Epstein, Jeffrey M
et al.

Publication Date

2020-05-29

DOI

10.1063/5.0006441

Peer reviewed

Time reversal symmetry breaking and odd viscosity in active fluids: Green-Kubo and NEMD results

Cory Hargus,[1,*] Katherine Klymko,[2] Jeffrey M. Epstein,[3] and Kranthi K. Mandadapu[1,4,†]

[1] *Department of Chemical and Biomolecular Engineering, University of California, Berkeley, CA, USA*
[2] *Computational Research Division, Lawrence Berkeley National Laboratory, Berkeley, CA, USA*
[3] *Department of Physics, University of California, Berkeley, CA, USA*
[4] *Chemical Sciences Division, Lawrence Berkeley National Laboratory, Berkeley, CA, USA*

Active fluids, which are driven at the microscale by non-conservative forces, are known to exhibit novel transport phenomena due to the breaking of time reversal symmetry. Recently, Epstein and Mandadapu [1] obtained Green-Kubo relations for the full set of viscous coefficients governing isotropic chiral active fluids, including the so-called odd viscosity, invoking Onsager's regression hypothesis for the decay of fluctuations in active non-equilibrium steady states. In this Communication, we test these Green-Kubo relations using molecular dynamics simulations of a canonical model system consisting of actively torqued dumbbells. We find the resulting odd and shear viscosity values from the Green-Kubo relations to be in good agreement with values measured independently through non-equilibrium molecular dynamics (NEMD) flow simulations. This provides a rigorous test of the Green-Kubo relations, and validates the application of the Onsager regression hypothesis in relation to viscous behaviors of active matter systems.

Introduction. Statistical physics has traditionally been concerned with systems at equilibrium. A natural generalization pursued by Onsager, Prigogine, de Groot and Mazur, and others is to consider systems that are globally out of equilibrium but that obey the local equilibrium hypothesis [2–6]. Such systems model transport phenomena allowing linear laws, such as those of Fourier and Fick, to be derived from the principles of equilibrium thermodynamics and statistical mechanics [4, 5, 7]. The physical origin of the non-equilibrium nature of these systems is driving at boundaries, as in a rod heated from one end or a channel connecting regions of different solute concentration.

A more radical departure from equilibrium is achieved in active matter systems, in which equilibrium is broken at the local level by non-conservative microscopic forces. Such activity is known to modify existing phase behavior as well as give rise to qualitatively new dynamical phases, as in motility-induced phase separation [9, 10]. Similarly, activity not only modifies existing transport coefficients, but can lead to entirely new coefficients, such as the odd (or Hall) viscosity appearing in chiral active fluids [1, 11–14].

Recent work by Epstein and Mandadapu [1] reveals that odd viscosity arises in two-dimensional chiral active fluids due to the breaking of time reversal symmetry at the level of stress correlations. This is demonstrated by a set of Green-Kubo relations derived through the application of the Onsager regression hypothesis [4, 5, 7]. In this Communication, we evaluate these Green-Kubo relations using molecular dynamics simulations of a model system composed of microscopically torqued dumbbells, finding them to be in good agreement with non-equilibrium molecular dynamics (NEMD) flow simulations across a wide range of densities and activities (Fig. 4).

Theory. We begin by reviewing the continuum theory in [1] for two-dimensional viscous active fluids with internal spin. This provides the setting for the derivation of Green-Kubo relations for viscosity coefficients in fluids breaking time reversal symmmetry. Because the chiral active dumbbell model considered in this paper is capable of storing angular momentum in the form of molecular or internal spin, we anticipate coupling between a velocity field v_i and a spin field m. These satisfy balance equations for linear and angular momentum, as proposed by Dahler and Scriven [15]:

$$\rho \dot{v}_i = T_{ij,j} + \rho g_i \,, \tag{1}$$

$$\rho \dot{m} = C_{i,i} - \epsilon_{ij} T_{ij} + \rho G \,. \tag{2}$$

T_{ij} denotes the stress tensor and C_i the spin flux, which accounts for transfer of internal angular momentum across surfaces. The variables g_i and G denote body forces and body torques, respectively. Finally note that the balance of angular momentum includes a term in which the two-dimensional Levi-Civita tensor ϵ_{ij} is contracted with the stress, so that the antisymmetric component of the stress may be nontrivial. We use the notation $a_{,i} = \partial a / \partial x_i$.

The most general isotropic constitutive equations for viscous fluids relating T_{ij} and C_i to v_i, m and their derivatives up to first order in two-dimensional systems

Authors' note: Independent and concurrently released work by Han *et al.* [8] measures transport coefficients including the odd viscosity in a model system consisting of frictional granular particles, upon obtaining identical Green-Kubo equations presented in [1] through a projection operator formalism. Together with the present work, this confirms the robustness and applicability of the Green-Kubo relations.

are given by

$$T_{ij} = \eta_{ijkl} v_{k,l} + \gamma_{ij} m - p\delta_{ij} + p^* \epsilon_{ij} \,, \tag{3}$$
$$C_i = \alpha_{ij} m_{,j} \,, \tag{4}$$

where η_{ijkl}, γ_{ij} and α_{ij} are the viscous transport coefficients [1]. Here, p and p^* are hydrostatic contributions and are not constitutively related to v_i and m. Isotropy further allows the transport coefficients to be constrained to have the form

$$\eta_{ijkl} = \sum_{n=1}^{6} \lambda_n s^{(n)}_{ijkl} \,, \tag{5}$$
$$\gamma_{ij} = \gamma_1 \delta_{ij} + \gamma_2 \epsilon_{ij} \,, \tag{6}$$
$$\alpha_{ij} = \alpha_1 \delta_{ij} + \alpha_2 \epsilon_{ij}. \tag{7}$$

This follows from a general representation theorem stating that any isotropic tensor can be expressed in a basis consisting of contractions of Kronecker tensors δ_{ij} and Levi-Civita tensors ϵ_{ij} and that, consequently, there exist no isotropic tensors of odd rank in two dimensions; see Ref. [1] for a detailed discussion and Appendix Table I for the definitions of tensors $s^{(n)}_{ijkl}$.

The coefficients γ_i and α_i indicate the responses of the stress and spin flux tensors to spin and spin gradients. λ_1 and λ_2 are the typical bulk and shear viscosities. λ_3 is the rotational viscosity indicating resistance to vorticity and giving rise to an anti-symmetric stress, while λ_4 is the so-called odd viscosity quantifying response to shear with a tension or compression in the orthogonal direction. λ_5 and λ_6 correspond to an anti-symmetric pressure from compression and isotropic pressure from vorticity, respectively. Note that non-vanishing λ_3 or λ_6 violates objectivity (independence of stress from vorticity), while non-vanishing λ_3 or λ_5 violates symmetry of the stress tensor.

Using the conservation and constitutive equations (1)-(2) and (5)-(7), Ref. [1] obtains a set of Green-Kubo relations for γ_n and λ_n via invocation of the Onsager regression hypothesis:

$$\gamma_1 = \frac{1}{2\rho_0 \nu} \delta_{ij} \epsilon_{kl} \mathcal{T}^{ijkl}, \tag{8}$$
$$\gamma_2 = \frac{1}{2\rho_0 \nu} \epsilon_{ij} \epsilon_{kl} \mathcal{T}^{ijkl}, \tag{9}$$
$$\lambda_1 + 2\lambda_2 + \lambda_3 - \frac{\gamma_1 \pi}{2\mu} + \frac{\gamma_2 \tau}{2\mu} = \frac{1}{2\rho_0 \mu} \delta_{ik} \delta_{jl} \mathcal{T}^{ijkl}, \tag{10}$$
$$\lambda_4 + \lambda_5 + \lambda_6 - \frac{\gamma_1 \tau}{4\mu} - \frac{\gamma_2 \pi}{4\mu} = \frac{1}{4\rho_0 \mu} \epsilon_{ik} \delta_{jl} \mathcal{T}^{ijkl}, \tag{11}$$
$$\lambda_5 - \frac{\gamma_2 \pi}{4\mu} = \frac{1}{8\rho_0 \mu} \epsilon_{ij} \delta_{kl} \mathcal{T}^{ijkl}, \tag{12}$$
$$\lambda_3 + \frac{\gamma_2 \tau}{2\mu} = \frac{1}{4\rho_0 \mu} \epsilon_{ij} \epsilon_{kl} \mathcal{T}^{ijkl} \,. \tag{13}$$

$\mathcal{T}^{ijkl}$ is the integrated stress correlation function given by

$$\mathcal{T}^{ijkl} = \int_0^\infty dt \langle \delta T_{ij}(t) \delta T_{kl}(0) \rangle. \tag{14}$$

μ, ν, τ, and π are static correlation functions in the non-equilibrium steady state given by

$$\mu \delta_{ij} = \frac{1}{L^4} \int \left\langle \delta v^i(\mathbf{x}) \delta v^j(\mathbf{y}) \right\rangle d^2\mathbf{x}\, d^2\mathbf{y} \,, \tag{15}$$
$$\pi = \frac{1}{L^4} \int (y^i - x^i) \left\langle \delta v^i(\mathbf{x}) \delta m(\mathbf{y}) \right\rangle d^2\mathbf{x}\, d^2\mathbf{y} \,, \tag{16}$$
$$\tau = \frac{1}{L^4} \int \epsilon_{kr} (y^r - x^r) \left\langle \delta m(\mathbf{x}) \delta v^k(\mathbf{y}) \right\rangle d^2\mathbf{x}\, d^2\mathbf{y} \,, \tag{17}$$
$$\nu = \frac{1}{L^4} \int \langle \delta m(\mathbf{x}) \delta m(\mathbf{y}) \rangle \, d^2\mathbf{x}\, d^2\mathbf{y} \,, \tag{18}$$

respectively. In particular, μ and ν can also be regarded as the effective translation and spin temperatures in the steady state. For equilibrium systems, equipartition implies $\mu = \nu$ and $\pi = \tau = 0$. Lastly, the above Green-Kubo relations show that two of the transport coefficients λ_3 and γ_2 are related by $2\lambda_3 = \gamma_2(\nu - \tau)/\mu$. Note that the stress tensor in (14) is defined as a spatial average, as in the following section, unlike the velocity and spin fields in (15)-(18).

For the chiral active dumbbell fluid, the situation is further simplified. As we will show in the following sections, the absence of alignment interactions between dumbbells results in $\gamma_1 = \gamma_2 = 0$, effectively decoupling the velocity from the spin field and also setting $\lambda_3 = 0$. Moreover, symmetry and objectivity of the stress tensor sets two more of the viscosity coefficients to zero, leaving

$$\begin{aligned} \eta_{ijkl} = \lambda_1 \big(\delta_{ij}\delta_{kl}\big) + \lambda_2 \big(\delta_{ik}\delta_{jl} - \epsilon_{ik}\epsilon_{jl}\big) \\ + \lambda_4 \big(\epsilon_{ik}\delta_{jl} + \epsilon_{jl}\delta_{ik}\big) \,. \end{aligned} \tag{19}$$

These simplifications also allow us to write simplified Green-Kubo expressions for the shear and odd viscosities

$$\begin{aligned} \lambda_2 = \frac{1}{4\rho_0 \mu} \int_0^\infty dt \, \langle (\delta T_{22}(t) - \delta T_{11}(t)) \\ (\delta T_{22}(0) - \delta T_{11}(0)) \rangle \,, \end{aligned} \tag{20}$$

and

$$\begin{aligned} \lambda_4 = \frac{1}{4\rho_0 \mu} \int_0^\infty dt \Big[\langle \delta T_{11}(t) \delta T_{21}(0) \rangle - \langle \delta T_{11}(0) \delta T_{21}(t) \rangle \\ + \langle \delta T_{12}(t) \delta T_{22}(0) \rangle - \langle \delta T_{12}(0) \delta T_{22}(t) \rangle \Big] \,, \end{aligned} \tag{21}$$

(see Appendix II for separating the coefficient λ_2 from (10)). Equation (21) shows that non-vanishing odd viscosity, *i.e.,* $\lambda_4 \neq 0$ requires breaking time reversal symmetry at the level of stress correlation functions, thus

breaking the Onsager reciprocal relations [1, 5]. Note that (20) is not the typical Green-Kubo expression used to calculate the shear viscosity. However, it can also be rewritten for isotropic systems in the typical form, which are invariant under rotation as

$$\lambda_2 = \frac{1}{\rho_0 \mu} \int_0^\infty dt \, \langle \delta T'_{12}(t) \delta T'_{12}(0) \rangle \,, \tag{22}$$

using a transformation $\boldsymbol{T'} = \boldsymbol{R^T T R}$ corresponding to a rotation tensor $\boldsymbol{R}$ of angle $\pi/4$, for which $T'_{12} = \frac{1}{2}(T_{22} - T_{11})$. The form in (20) is a result of the theory for the choice of the representation theorem for viscous transport coefficients using the basis $s^{(n)}_{ijkl}$.

In what follows, we evaluate the shear and odd viscosity Green-Kubo expressions at various densities and driving forces by using molecular simulations of chiral active dumbbells in a non-equilibrium steady state. We then subject the dumbbell system to imposed periodic-Poiseulle simulations [16] resulting in non-uniform shearing flows, and evaluate the shear and viscous coefficients independently. Such an analysis will provide support to both the application of Onsager's regression hypothesis to fluctuations in active non-equilibrium steady states and the ensuing Green-Kubo relations for viscous behaviors of active systems.

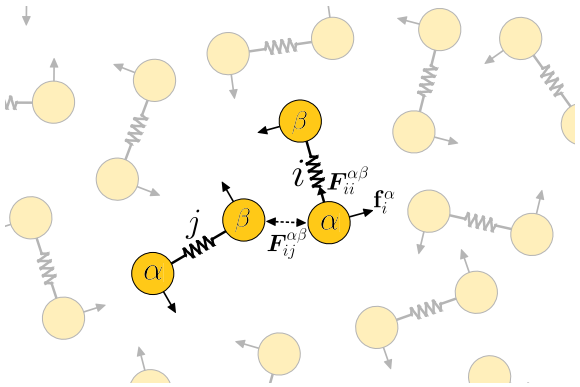

FIG. 1. A two-dimensional fluid composed of chiral active dumbbells. In addition to interacting with its neighbors, each dumbbell is rotated counterclockwise by equal and opposite active forces $\mathbf{f}^\alpha_i$.

Microscopic model–Chiral active dumbbells. We consider a fluid composed of dumbbells subject to active torques [17], as shown in Fig. 1. Each dumbbell is composed of two particles of unit mass connected by a harmonic spring. The system evolves according to underdamped Langevin dynamics

$$\begin{aligned} \dot{\boldsymbol{x}}^\alpha_i &= \boldsymbol{v}^\alpha_i \,, \\ \dot{\boldsymbol{v}}^\alpha_i &= \sum_{j\beta} \boldsymbol{F}^{\alpha\beta}_{ij} + \mathbf{f}^\alpha_i + \boldsymbol{g}^\alpha_i - \gamma \boldsymbol{v}^\alpha_i \\ &\qquad + \sqrt{2\gamma k_\mathrm{B} T} \frac{d\boldsymbol{W}^\alpha_i}{dt} \,, \end{aligned} \tag{23}$$

with indices $i, j \in [1, N]$ and $\alpha, \beta \in \{1, 2\}$ running over dumbbells and particles, respectively. Variables $\boldsymbol{x}^\alpha_i$ and $\boldsymbol{v}^\alpha_i$ represent atom positions and velocities. γ is the dissipative substrate friction and T the substrate temperature determining the variance of the thermal fluctuations $\frac{d\boldsymbol{W}^\alpha_i}{dt}$, modeled as Gaussian white noise. Particles in different dumbbells interact through a pairwise WCA potential [18], resulting in interaction forces $\boldsymbol{F}^{\alpha\beta}_{ij}$. The particles in a dumbbell are subjected to equal and opposite non-conservative active forces $\mathbf{f}^\alpha_i$, which satisfy $\mathbf{f}^1_i = -\mathbf{f}^2_i := \mathbf{f}_i$, and are always perpendicular to the bond vector $\boldsymbol{d}_i = \boldsymbol{x}^1_i - \boldsymbol{x}^2_i$. This imposes an active torque at the level of individual dumbbells. Finally, $\boldsymbol{g}^\alpha_i = \boldsymbol{g}(\boldsymbol{x}^\alpha_i)$ is an optional externally imposed body force, and will be employed later in Poisueille flow simulations to test the Green-Kubo relations.

Previous work [17] used the Irving-Kirkwood procedure to coarse-grain the microscopic equations (23) and derive the equations of hydrodynamics, including balance of mass, linear momentum and angular momentum, as also employed in the context of measuring odd viscosity by [14]. This coarse-graining procedure yields expressions for the stress tensor in terms of molecular variables and active forces. In particular, it is found that applying active couple forces at the microscale results in an asymmetric stress tensor given by

$$\boldsymbol{T} = \boldsymbol{T}^\mathrm{K} + \boldsymbol{T}^\mathrm{V} + \boldsymbol{T}^\mathrm{A} \,, \tag{24}$$

where

$$\boldsymbol{T}^\mathrm{K} = -\frac{1}{A} \sum_{i,\alpha} m^\alpha_i \boldsymbol{v}^\alpha_i \otimes \boldsymbol{v}^\alpha_i \,, \tag{25}$$

$$\boldsymbol{T}^\mathrm{V} = -\frac{1}{2A} \sum_{i,j,\alpha,\beta} \boldsymbol{F}^{\alpha\beta}_{ij} \otimes \boldsymbol{x}^{\alpha\beta}_{ij} \,, \tag{26}$$

$$\boldsymbol{T}^\mathrm{A} = -\frac{1}{A} \sum_{i} \mathbf{f}_i \otimes \boldsymbol{d}_i \,, \tag{27}$$

denote the kinetic, virial, and active contributions, respectively.

The active force vector $\mathbf{f}_i$ is related to the unit bond vector $\hat{\boldsymbol{d}}_i$ by a rotation matrix $\boldsymbol{R}$ of angle $\pi/2$, *i.e.,*

$$\mathbf{f}_i = \mathrm{f} \boldsymbol{R} \hat{\boldsymbol{d}}_i \tag{28}$$

For positive (negative) f, the dumbbells rotate counterclockwise (clockwise). We find that the steady state time average of $\boldsymbol{T^A}$ is

$$\begin{aligned} \langle \boldsymbol{T^A} \rangle &= -\rho_0 \langle \mathbf{f} \otimes \boldsymbol{d} \rangle \\ &= -\rho_0 \mathrm{f} d \langle \boldsymbol{R} \hat{\boldsymbol{d}} \otimes \hat{\boldsymbol{d}} \rangle = \frac{\rho_0 \mathrm{f} d}{2} \begin{bmatrix} 0 & 1 \\ -1 & 0 \end{bmatrix} , \end{aligned} \tag{29}$$

where $d = \langle |\boldsymbol{d}| \rangle$ is the average bond length. Because the dumbbells rotate with no preferred alignment, the antisymmetry of $\langle \boldsymbol{T^A} \rangle$ follows from replacing the time

average with a uniformly weighted average over angles of rotation θ. For example,

$$\langle \boldsymbol{R}\hat{\boldsymbol{d}} \otimes \hat{\boldsymbol{d}} \rangle_{21} = \langle \hat{d}_1 \hat{d}_1 \rangle = \frac{1}{2\pi} \int_0^{2\pi} d\theta \ \cos^2(\theta) = \frac{1}{2} \quad (30)$$

while the diagonal elements are zero. This shows that the antisymmetric hydrostatic-like term p^* introduced in (3) arises in a non-equilibrium steady state of the active dumbbell model due to the presence of active rotational forces, and has the magnitude $p^* = \rho_0 \mathrm{f} d/2$. We further relate p^* to a non-dimensional Péclet number describing the ratio of active rotational forces to thermal fluctuations due to the substrate bath

$$\mathrm{Pe} = \frac{2\mathrm{f}d}{\rho_0 \mu} = \frac{4p^*}{\mu \rho_0^2}. \quad (31)$$

We use Pe as defined in (31) to vary the activity in the system when evaluating the transport coeffcients.

Green-Kubo calculations. Steady-state molecular dynamics simulations allow direct measurement of the integrated stress correlation functions $\mathcal{T}_{ijkl}$ defined in (14), which are required for evaluation of the viscous transport coefficients using the Green-Kubo equations (8)-(13). We find that several of these coefficients vanish in the non-equilibrium steady states at all simulated activities and densities due to cancellations of the correlation functions (see Appendix Fig. 5). In particular,

$$\epsilon_{ij}\epsilon_{kl}\mathcal{T}_{ijkl} = \delta_{ij}\epsilon_{kl}\mathcal{T}_{ijkl} = \epsilon_{ij}\delta_{kl}\mathcal{T}_{ijkl} = 0\,. \quad (32)$$

This immediately implies $\gamma_1 = \gamma_2 = \lambda_3 = \lambda_5 = \lambda_6 = 0$, so that the stress tensor is symmetric and objective. It now remains to evaluate the two non-trivial transport coefficients λ_2 and λ_4 using (20) and (21).

Figure 2 shows the stress correlators $\langle \delta T_{11}(t) \delta T_{21}(0) \rangle$ and $\langle \delta T_{11}(0) \delta T_{21}(t) \rangle$ for various Pe. These are typically zero for systems in equilibrium, and become non-zero whenever $\mathrm{Pe} \neq 0$. In particular, we find these correlation functions to be equal and opposite, and therefore add constructively yielding a non-vanishing odd viscosity from the Green-Kubo relation (21). In general, for the chiral active dumbbell fluid, we find

$$\begin{aligned} \langle \delta T_{11}(t) \delta T_{21}(0) \rangle &= -\langle \delta T_{11}(0) \delta T_{21}(t) \rangle \\ &= -\langle \delta T_{11}(\text{-}t) \delta T_{21}(0) \rangle\,, \end{aligned} \quad (33)$$

where the final equality is due to stationarity. The analogous equations are satisfied by $\langle \delta T_{12}(t) \delta T_{22}(0) \rangle$.

Figure 4 shows the Green-Kubo estimates for λ_2 and λ_4 for various activities and for a range of low to high densities. We find that the shear viscosity increases with density as well as with activity. The dependence of the odd viscosity on activity, while apparently linear at low density, becomes increasingly sigmoidal at high density. Note that the odd viscosity, as a non-dissipative transport coefficient, may be negative without introducing an inconsistency with the second law of thermodynamics.

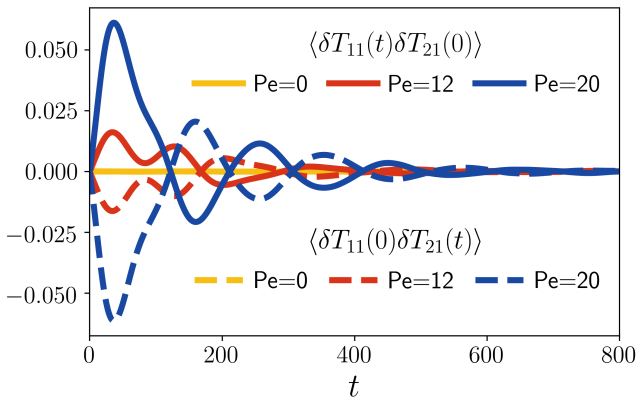

FIG. 2. Stress correlation functions contributing to the odd viscosity ($\rho_0 = 0.4$). For $\mathrm{Pe} \neq 0$ these correlation functions add constructively, yielding a nonzero odd viscosity.

Poiseuille flow NEMD simulations. To verify the values computed from the Green-Kubo formulas, (20) and (21), we measure λ_2 and λ_4 independently via non-equilibrium molecular dynamics simulations. To this end, we simulate plane Poiseuille-like flow via the inclusion of a nonzero body force $\boldsymbol{g}$ in (23) according to the periodic Poiseuille method [16]. We apply equal and opposite body forces as shown in Fig. 3, of magnitude g_1 in the x_1 direction compatible with periodic boundary conditions.

This setup represents a non-trivial boundary value problem, which not only yields non-uniform flows and non-uniform stresses, but also provides a stringent test for the expected constitutive behaviors of the active dumbbell fluid and the estimates of the transport coefficients obtained from Green-Kubo formulas. The velocity profile and pressure profiles for such an applied body

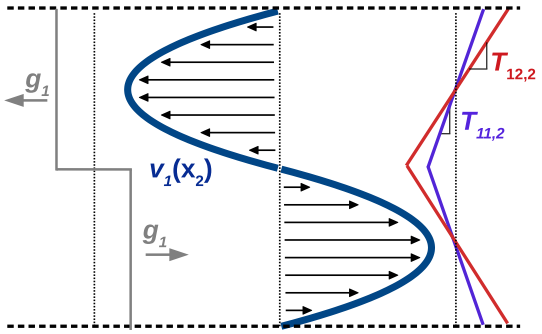

FIG. 3. A schematic of the periodic Poiseuille non-equilibrium molecular dynamics (NEMD) simulation method. The top half of the system is subjected to a uniform body force to the left, and the bottom half to a uniform body force of equal magnitude to the right. This yields a parabolic velocity profile and, for odd viscous fluids, an atypical normal stress.

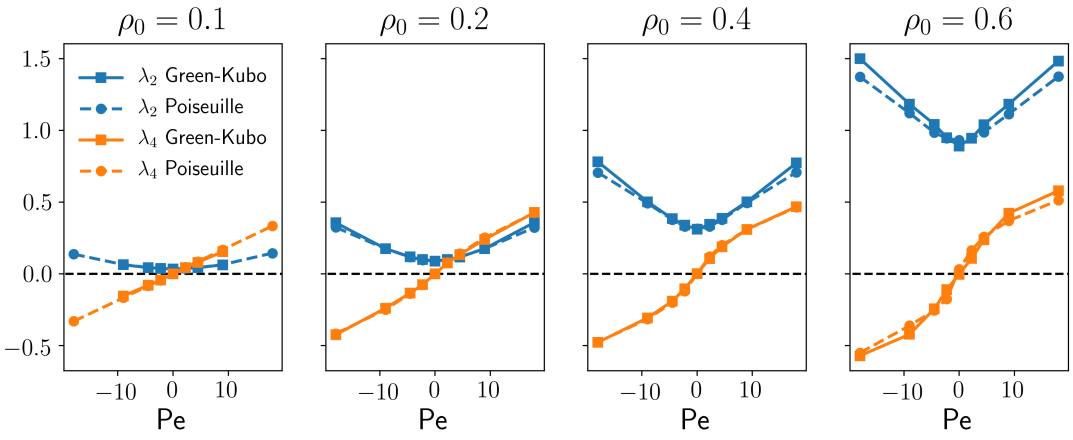

FIG. 4. Comparison of shear viscosity (λ_2) and odd viscosity (λ_4) values obtained from the Green-Kubo relations with those obtained from periodic Poiseuille NEMD simulations, showing agreement across a range of activities and densities.

force can be solved analytically and are given by

$$v_1(x_2) = \frac{\rho_0 g_1}{2\lambda_2} x_2(L - x_2)\,, \tag{34}$$

and

$$p(x_2) = \frac{\lambda_4}{\lambda_2}\rho_0 g_1 x_2 + p_0\,, \tag{35}$$

respectively, where p_0 is an arbitrary reference pressure (see Appendix IV for the solution to the corresponding boundary value problem). Our simulations of active dumbbell fluids are consistent with these profiles for various densities and activities. Given the velocity and pressure profiles in (34) and (35), the shear and odd viscosities can be computed from the expressions

$$\lambda_2 = \frac{\rho_0 g_1 L^2}{12\bar{v}}\,, \tag{36}$$

$$\lambda_4 = \frac{T_{11,2}}{2v_{1,22}} = -\frac{\lambda_2 T_{11,2}}{2\rho_0 g_1}\,, \tag{37}$$

respectively, where $\bar{v} = \frac{1}{L}\int_0^L dx_2\ v_1(x_2)$; see Appendix IV. The slope of the stress component T_{11} can be identified in molecular simulations using the Irving-Kirkwood expression (24)-(27).

The shear and odd viscosities calculated using this NEMD approach are in excellent agreement with the Green-Kubo predictions for a wide range of densities and Péclet numbers, see Fig. 4.

Discussion. In this work, we have validated the non-equilibrium Green-Kubo formulas derived in [1], showing that the odd viscosity results directly from the breaking of time reversal symmetry at the level of stress fluctuations in the steady state. In doing so, we also provide support for the application of the Onsager regression hypothesis to fluctuations about the non-equilibrium steady state, which was used to derive these equations. Future work entails understanding the microscopic origins of the functional dependence of the viscosities with density and activity.

Acknowledgements. C.H. is supported by the National Science Foundation Graduate Research Fellowship Program under Grant No. DGE 1752814. K.K.M is supported by Director, Office of Science, Office of Basic Energy Sciences, of the U.S. Department of Energy under contract No. DEAC02-05CH11231.

* hargus@berkeley.edu
† kranthi@berkeley.edu

[1] J. M. Epstein and K. K. Mandadapu, arXiv:1907.10041 (2019).
[2] S. R. de Groot, *Thermodynamics of Irreversible Processes* (Interscience Publishers Inc., New York, 1951).
[3] S. R. de Groot and P. Mazur, *Non-Equilibrium Thermodynamics* (Dover, New York, 1984).
[4] L. Onsager, Physical review **37**, 405 (1931).
[5] L. Onsager, Physical review **38**, 2265 (1931).
[6] I. Prigogine, *Introduction to Thermodynamics of Irreversible Processes* (Wiley-Interscience, New York, 1967).
[7] R. Kubo, M. Yokota, and S. Nakajima, Journal of physical society of Japan **12**, 1203 (1957).
[8] M. Han, M. Fruchart, C. Scheibner, S. Vaikuntanathan, W. Irvine, J. de Pablo, and V. Vitelli, arXiv preprint arXiv:2002.07679 (2020).
[9] J. Tailleur and M. E. Cates, Physical review letters **100**, 218103 (2008).
[10] M. E. Cates and J. Tailleur, Annual reviews of condense matter physics **6**, 219 (2015).
[11] D. Banerjee, A. Souslov, A. G. Abanov, and V. Vitelli, Nature communications **8**, 1573 (2017).
[12] S. Ganeshan and A. G. Abanov, Physical review fluids **2**, 094101 (2017).
[13] A. Souslov, K. Dasbiswas, M. Fruchart, S. Vaikun-

tanathan, and V. Vitelli, Physical review letters **122**, 128001 (2019).
[14] Z. Liao, M. Han, M. Fruchart, V. Vitelli, and S. Vaikuntanathan, The Journal of chemical physics **151**, 194108 (2019).
[15] J. Dahler and L. Scriven, Nature **192**, 36 (1961).
[16] J. A. Backer, C. P. Lowe, H. C. Hoefsloot, and P. D. Iedema, The journal of chemical physics **122** (2005).
[17] K. Klymko, D. Mandal, and K. K. Mandadapu, The Journal of chemical physics **147**, 194109 (2017).
[18] J. D. Weeks, D. Chandler, and H. C. Andersen, The journal of chemical physics **54**, 5237 (1971).
[19] S. J. Plimpton, J. Comp. Phys. **117**, 1 (1995), see also http://lammps.sandia.gov/.

Appendix

I. Simulation Details

To investigate the viscous behavior of a fluid composed of self-spinning dumbbells, we perform molecular dynamics simulations in LAMMPS [19], implementing our own modifications [1] to impose microscopic driving forces and compute the active stress $\boldsymbol{T}^{\mathrm{A}}$. Particles interact with their non-bonded neighbors through a Weeks-Chandler-Andersen [18] potential defined by

$$V_{ij}^{\mathrm{WCA}}(r) = \begin{cases} 4\epsilon\left[\left(\sigma/r\right)^{12} - \left(\sigma/r\right)^{6}\right] + \epsilon & r < 2^{1/6}\sigma \\ 0 & r \geq 2^{1/6}\sigma\,. \end{cases}$$

Here, σ, ϵ and particle mass m are the characteristic length, energy, and mass scales, which are used to define the Lennard-Jones units system. All numerical settings and results in this Communication are reported in Lennard-Jones units. The two particles in a single dumbbell are held together by a harmonic potential $V(r) = \frac{1}{2}k(r - r_0)^2$ with spring constant $k = 100$ and reference length $r_0 = 1$.

Dynamics are evolved according to underdamped Langevin dynamics (23) with bath temperature $T = 1.0$ and friction $\gamma = 0.5$. We apply the Langevin bath interactions only along the x_2 direction, so as not to impede flow in the x_1 direction, and employ these conditions in both Green-Kubo and periodic Poiseuille simulations. We note that imposing bath interactions selectively along x_2 may lead to a violation of isotropy by aligning dumbbells along a preferred axis. In all simulations, however, we check that dumbbells have no preferred alignment by measuring the departure of the bond angle of a dumbbell projected onto $[0, \pi/2]$ from the reference value of $\pi/4$:

$$\delta\theta_i^+ = \arctan\left(\frac{|\mathbf{d}_i \cdot \mathbf{e}_2|}{|\mathbf{d}_i \cdot \mathbf{e}_1|}\right) - \frac{\pi}{4}\,. \tag{38}$$

We find that in all simulations, $\max(|\langle\delta\theta_i^+\rangle|) < 0.01$ radians, where angle brackets indicate averaging in time and the maximum is over all dumbbells. We also confirm that the density is indeed uniform in all periodic Poiseuille calculations. The relative spatial variation in the density is bounded in all simulations by $\left(\langle(\delta\rho)^2\rangle/\langle\rho^2\rangle\right)^{1/2} < 0.1\%$.

II. Green-Kubo Formula for Shear Viscosity

In Table I, we provide the basis for the 2D viscosity tensor η_{ijkl} derived in [1]. We also perform a derivation to obtain separate expressions for the shear and bulk viscosities. To this end, we begin with the following equation (also equation (127) in SI of [1] in the absence of internal spin):

$$k^j k^l \eta_{ijkl} = \frac{1}{\rho_0 \mu} k^j k^l \int_0^\infty dt\ \langle \delta T_{\mathbf{k}}^{ij}(t) \delta T_{-\mathbf{k}}^{kl}(0)\rangle = \frac{1}{\rho_0 \mu} k^j k^l \mathcal{T}_{ijkl}^{\mathbf{k}}\,, \tag{39}$$

where

$$\mathcal{T}_{ijkl}^{\mathbf{k}} = \int_0^\infty dt\ \langle \delta T_{\mathbf{k}}^{ij}(t) \delta T_{-\mathbf{k}}^{kl}(0)\rangle\,. \tag{40}$$

Following [1], we can obtain an equation for λ_1 and λ_2

$$\lambda_1 + 2\lambda_2 = \frac{1}{2\rho_0 \mu} \delta_{ik}\delta_{jk} \mathcal{T}_{ijkl}^{\mathbf{k}}\,, \tag{41}$$

in the limit of $\mathbf{k} \to \mathbf{0}$.

---

[1] Our simulation and analysis code is publicly available at https://github.com/mandadapu-group/active-matter

Basis Tensor	Components	$i \leftrightarrow j$	$k \leftrightarrow l$	$ij \leftrightarrow kl$	P
$\mathbf{s}^{(1)}$	$\delta_{ij}\delta_{kl}$	+	+	+	+
$\mathbf{s}^{(2)}$	$\delta_{ik}\delta_{jl} - \epsilon_{ik}\epsilon_{jl}$	+	+	+	+
$\mathbf{s}^{(3)}$	$\epsilon_{ij}\epsilon_{kl}$	-	-	+	+
$\mathbf{s}^{(4)}$	$\epsilon_{ik}\delta_{jl} + \epsilon_{jl}\delta_{ik}$	+	+	-	-
$\mathbf{s}^{(5)}$	$\epsilon_{ik}\delta_{jl} - \epsilon_{jl}\delta_{ik} + \epsilon_{ij}\delta_{kl} + \epsilon_{kl}\delta_{ij}$	-	+	N/A	-
$\mathbf{s}^{(6)}$	$\epsilon_{ik}\delta_{jl} - \epsilon_{jl}\delta_{ik} - \epsilon_{ij}\delta_{kl} - \epsilon_{kl}\delta_{ij}$	+	-	N/A	-

TABLE I. Basis for the isotropic rank four tensors in two dimensions corresponding to viscous transport coefficients η_{ijkl}. We also indicate the nature of the tensors under index permutations (A) $i \leftrightarrow j$ indicating the symmetry of the stress tensor, (B) $k \leftrightarrow l$ indicating objectivity, (C) $i \leftrightarrow k$, $j \leftrightarrow l$, indicating symmetry with respect to Onsager reciprocal relations, and finally (D) the mirror transformation $x_1 \mapsto -x_1$, $x_2 \mapsto x_2$, also known as parity transformation (P). Reproduced from [1].

To separate λ_1 from λ_2 we return to (39) and contract both sides with $k^i k^k$ to obtain

$$k^i k^j k^k k^l \eta_{ijkl} = \frac{1}{\rho_0 \mu} k^i k^j k^k k^l \mathcal{T}^{\mathbf{k}}_{ijkl} \,. \tag{42}$$

The resulting equation holds independently for any choice of $\mathbf{k}$ in the limit $\mathbf{k} \to 0$. Now, we set $\mathbf{k} = k(\mathbf{e}_1 + \mathbf{e}_2)$ and $\mathbf{k} = k(\mathbf{e}_1 - \mathbf{e}_2)$ in (42) and sum the resulting equations to obtain

$$4\lambda_1 + 4\lambda_2 = \frac{1}{\rho_0 \mu}\left(\mathcal{T}^{\mathbf{k}}_{1111} + \mathcal{T}^{\mathbf{k}}_{1122} + \mathcal{T}^{\mathbf{k}}_{1212} + \mathcal{T}^{\mathbf{k}}_{1221} + \mathcal{T}^{\mathbf{k}}_{2112} + \mathcal{T}^{\mathbf{k}}_{2121} + \mathcal{T}^{\mathbf{k}}_{2211} + \mathcal{T}^{\mathbf{k}}_{2222}\right), \tag{43}$$

which cannot be written in compact form as a contraction of Kronecker and Levi-Civita tensors with $\mathcal{T}^{\mathbf{k}}_{ijkl}$. Subtracting (43) from twice (41) and invoking the symmetry of the stress fluctuations gives

$$\begin{aligned} \lambda_2 &= \frac{1}{4\rho_0 \mu}(\mathcal{T}^{\mathbf{k}}_{1111} - \mathcal{T}^{\mathbf{k}}_{1122} - \mathcal{T}^{\mathbf{k}}_{2211} + \mathcal{T}^{\mathbf{k}}_{2222} + \mathcal{T}^{\mathbf{k}}_{1212} - \mathcal{T}^{\mathbf{k}}_{1221} - \mathcal{T}^{\mathbf{k}}_{2112} + \mathcal{T}^{\mathbf{k}}_{2121}) \\ &= \frac{1}{4\rho_0 \mu}(\mathcal{T}^{\mathbf{k}}_{1111} - \mathcal{T}^{\mathbf{k}}_{1122} - \mathcal{T}^{\mathbf{k}}_{2211} + \mathcal{T}^{\mathbf{k}}_{2222}) \,. \end{aligned} \tag{44}$$

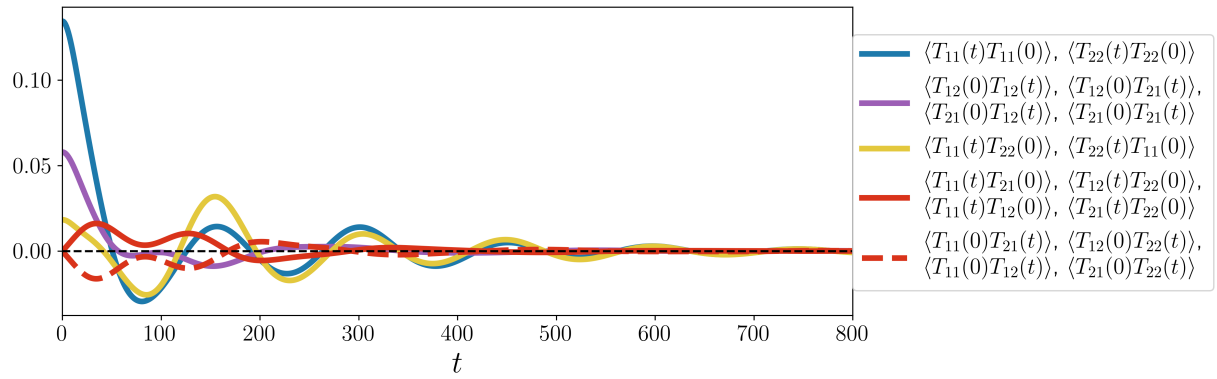

FIG. 5. The sixteen stress correlation functions computed at $\rho_0 = 0.4$, Pe $= 12$. Due to symmetries present in the chiral active dumbbell model, many of the correlation functions are identical, and are grouped as such. From this grouping, it is possible to ascertain that certain viscosity coefficients defined in (8)-(13) will vanish. For example, λ_3 depends on a sum of the correlation functions $\mathcal{T}_{1212} - \mathcal{T}_{1221} - \mathcal{T}_{2112} + \mathcal{T}_{2121}$. Here we see that these four correlation functions are identical, hence their sum will be zero. We further observe that the correlation functions contributing to the odd viscosity λ_4 go to zero in the static limit $t \to 0$, a consequence of the antisymmetry identified in (33).

Finally, returning to the definition of $\mathcal{T}^{\mathbf{k}}_{ijkl}$ in (39), and taking the zero wavevector limit $\mathbf{k} \to 0$ yields

$$\begin{aligned}\lambda_2 &= \frac{1}{4\rho_0\mu}\int_0^\infty dt\ \langle(\delta T_{22}(t) - \delta T_{11}(t))(\delta T_{22}(0) - \delta T_{11}(0))\rangle \\ &= \frac{1}{\rho_0\mu}\int_0^\infty dt\ \langle \delta T_{12}(t)\delta T_{12}(0)\rangle\,,\end{aligned} \tag{45}$$

where, in obtaining the last equality, we use material isotropy to make the stress transformation $\boldsymbol{T'} = \boldsymbol{R^T T R}$ corresponding to a two-dimensional rotation tensor $\boldsymbol{R}$ of angle $\pi/4$, for which $T'_{12} = \frac{1}{2}(T_{22} - T_{11})$. The last equality in (45) is the standard Green-Kubo relation for the shear viscosity. One may evaluate either of these expressions to compute the shear viscosity λ_2.

III. Decomposed contributions to the viscosity coefficients from the Irving-Kirkwood stress tensor

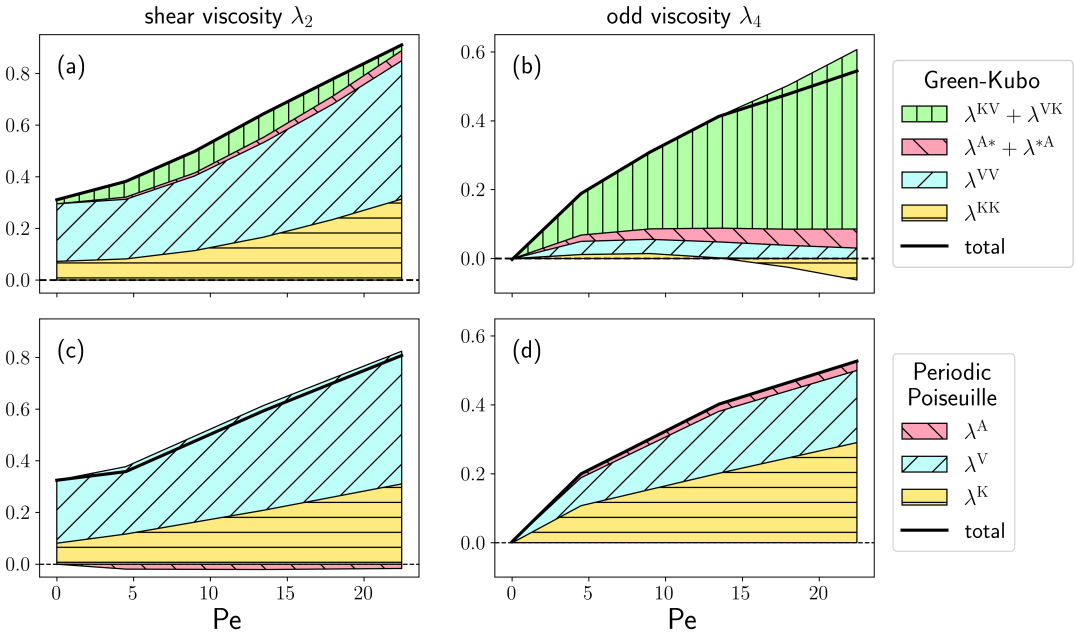

FIG. 6. Components of the stress contributing to Green-Kubo and Poiseuille calculations of the shear and odd viscosity at $\rho_0 = 0.4$ as a function of Pe. Figures (a) and (b) are the component-wise contributions to λ_2 and λ_4, respectively, from Green-Kubo calculations according to the decompositions in (46) and (47). Here, $\lambda^{A*} = \lambda^{AK} + \lambda^{AV} + \lambda^{AA}$ and similarly $\lambda^{*A} = \lambda^{KA} + \lambda^{VA} + \lambda^{AA}$. Figures (c) and (d) are the component-wise contributions to the λ_2 and λ_4, respectively, in periodic Poiseuille calculations. The solid black line indicates the total viscosity coefficient, obtained by adding the shaded areas above $y = 0$ and subtracting those below $y = 0$.

The Irving-Kirkwood procedure provides a natural decomposition of the stress tensor into kinetic, virial, and active molecular contributions (24). In Fig. 6, we examine the component-wise stress contributions to the shear and odd viscosity in both Green-Kubo and periodic Poiseuille calculations. The stress appears twice in the correlation functions entering the Green-Kubo equations *via* (14), thus there are nine components contributing to the Green-Kubo viscosity coefficients, which we label λ^{KK}, λ^{KV}, λ^{KA}, λ^{VK}, λ^{VV}, λ^{VA}, λ^{AK}, λ^{AV} and λ^{AA}.

From (20), we define a decomposed shear viscosity as

$$\lambda_2^{XY} = \frac{1}{\rho_0\mu}\int_0^\infty dt\ \langle \delta T^X_{12}(t)\delta T^Y_{12}(0)\rangle\,, \tag{46}$$

where $X, Y \in \{\mathrm{K}, \mathrm{V}, \mathrm{A}\}$ indicate the kinetic, virial and active parts. Similarly, the odd viscosity from (21) may be decomposed as

$$\lambda_4^{XY} = \frac{1}{4\rho_0\mu}\int_0^\infty dt\ \langle \delta T^X_{ij}(t)\delta T^Y_{kl}(0)\rangle\epsilon_{ik}\delta_{jl}\,. \tag{47}$$

For periodic Poiseuille calculations, the decompositions contributing to the viscous coefficients simply involve the choice of whether to use $\boldsymbol{T}^{\mathrm{K}}$, $\boldsymbol{T}^{\mathrm{V}}$, or $\boldsymbol{T}^{\mathrm{A}}$ in (36) and (37), corresponding to λ^{K}, λ^{V}, and λ^{A}, respectively. We observe that the active stress $\boldsymbol{T}^{\mathrm{A}}$ plays a small but not insignificant role in both λ_2 and λ_4 at $\mathrm{Pe} \neq 0$. Notably, the dominant Green-Kubo contributions to λ_2 are λ^{KK} and λ^{VV} while the cross correlations λ^{KV} and λ^{VK} are dominant in λ_4.

IV. Periodic Poiseuille Simulation

Non-equilibrium molecular dynamics simulations allow measurement of viscosity coefficients in direct analogy to experimental viscometry. For the chiral active dumbbell fluid, $\gamma_1 = \gamma_2 = \lambda_3 = \lambda_5 = \lambda_6 = 0$, resulting in decoupling of the linear and angular momentum balances and leading to modified Navier-Stokes equations

$$\rho \dot{v}_i = \lambda_1 v_{k,ki} + \lambda_2 v_{i,jj} + \lambda_4 \epsilon_{ik} v_{k,jj} - p_{,i} + \epsilon_{ij} p^*_{,j} + \rho g_i \,, \tag{48}$$

with bulk viscosity λ_1, shear viscosity λ_2, odd viscosity λ_4, pressure p, and body force g_i.

In the periodic Poiseuille simulations, we subject the system to equal and opposite body forces along the x_2 direction as shown in Fig. 3. In this case, we verify that the density ρ is well-approximated as constant for small shear rates, as described in Appendix I. Therefore, we assume incompressible flow,

$$v_{i,i} = 0 \,. \tag{49}$$

and obtain the simplified constitutive and Navier-Stokes equations:

$$T_{ij} = \lambda_2 \big(v_{i,j} + v_{j,i}\big) + \lambda_4 \big(\epsilon_{ik} v_{k,j} + \epsilon_{jk} v_{i,k}\big) - p\delta_{ij} + p^* \epsilon_{ij} \,, \tag{50}$$

and

$$\rho_0 v_{i,j} v_j = \lambda_2 v_{i,jj} + \lambda_4 \epsilon_{ik} v_{k,jj} - p_{,i} + \epsilon_{ij} p^*_{,j} + \rho_0 g_i \,. \tag{51}$$

where ρ_0 is the uniform reference density.

We now seek a steady state analytical solution for the velocity and pressure profiles of a fluid between two plates separated by a distance L, subjected to a body force $\mathbf{g} = (g_1, 0)$, where g_1 is uniform in space. The solution is analogous to that of a planar Poiseuille flow, with boundary conditions $v_i = 0$ at $x_2 = 0$ and $x_2 = L$. Using the ansatz $v_1 = v_1(x_2)$, $v_2 = 0$, $p = p(x_2)$, and $p^* = \text{const}$, one may find the steady state solution to be

$$v_1(x_2) = \frac{\rho_0 g_1}{2\lambda_2} x_2 (L - x_2) \,, \tag{52}$$

and

$$p(x_2) = \frac{\lambda_4}{\lambda_2} \rho_0 g_1 x_2 + p_0 \,, \tag{53}$$

where p_0 is an arbitrary reference pressure.

We see that the steady state velocity profile is identical to the usual solution for planar Poiseuille flow, remaining unaffected by odd viscosity. In fact it is always true that odd viscosity does not appear in the velocity profile in incompressible flows with no-slip boundary conditions [12]. The odd viscosity does appear, however, in a pressure gradient arising in the x_2-direction to maintain the no-penetration condition at the walls, *i.e.* to prevent flow in the x_2-direction. Our active dumbbell fluid simulations show parabolic velocity profiles consistent with (52) and (53) when subjected to equal and opposite body forces as shown in Fig. 3.

Integrating the velocity profile to get an average velocity $\bar{v} = \dfrac{1}{L}\int_0^L v_1(x_2) dx_2$, we obtain a convenient expression for computing the shear viscosity λ_2 in molecular simulations:

$$\lambda_2 = \frac{\rho_0 g_1 L^2}{12 \bar{v}} \,. \tag{54}$$

As noted above, λ_4 does not appear in the velocity but in the stress (50). For the velocity profile (52),

$$T_{11} = -p + \lambda_4 v_{1,2} \,, \tag{55}$$

which results in

$$T_{11,2} = -p_{,2} + \lambda_4 v_{1,22}\,. \tag{56}$$

Using (51) in the x_2-direction, one may reduce (56) to

$$T_{11,2} = 2\lambda_4 v_{1,22} = -2\lambda_4 \frac{\rho_0 g_1}{\lambda_2}\,. \tag{57}$$

Finally, rearranging (57), λ_4 is obtained in terms of the slope of T_{11} as

$$\lambda_4 = \frac{T_{11,2}}{2v_{1,22}} = -\frac{\lambda_2 T_{11,2}}{2\rho_0 g_1}\,. \tag{58}$$

where T_{11} can be calculated using the Irving-Kirkwood formula (24) for the active dumbbell fluid.